

Electronic Supporting Information

Harnessing Near-Infrared Light via S_0 to T_1 Sensitizer Excitation in a Molecular Photon Upconversion Solar Cell

*Drake Beery, Ashley Arcidiacono, Jonathan P. Wheeler, Jiaqi Chen, and Kenneth Hanson**

Department of Chemistry & Biochemistry, Florida State University, Tallahassee, Florida 32306, United States

Contents

1. A materials and synthesis.....	Page S2
2. Photophysical and Electrochemical Measurements.....	Page S5
3. Energy Level Calculations.....	Page S9
4. Figure S2. A photophysical data in DMSO	Page S9
5. Figure S3. Os photophysical data in DMSO	Page S10
6. Figure S4. ATR-FTIR absorbance spectra of TiO_2 - A films w and w/o Zn^{2+}	Page S10
7. Figure S5. A and Os loading isotherms on TiO_2	Page S11
8. Figure S6. Absorption spectra of bilayer films on TiO_2 w and w/o Zn^{2+}	Page S11
9. Figure S7. IPCE and absorptance of TiO_2 - A device	Page S12
10. Figure S8. IPCE and absorptance of TiO_2 - B-Zn-Os device	Page S12
11. Figure S9. IPCE and absorptance of TiO_2 - A-Zn-Os device.....	Page S13
12. Figure S10. IPCE of monolayer and bilayer devices.....	Page S13
13. Figure S11. J_{SC} vs. excitation intensity in mW/cm^2	Page S14
14. Figure S12. Absorption spectra of monolayer and bilayer films on ZrO_2	Page S14
15. Figure S13. Transient absorption spectra of Os in DMSO.....	Page S15
16. Figure S14. Transient absorption spectra of Os on TiO_2	Page S15
17. Figure S15. Transient absorption spectra of Os in TiO_2 - B-Zn-Os films.....	Page S16
18. Figure S16. Transient absorption spectra of A in DMSO.....	Page S16
19. Figure S17. Photophysical data of ZrO_2 - A films.....	Page S17
20. References.....	Page S17

Materials and Synthesis

Synthesis of A:

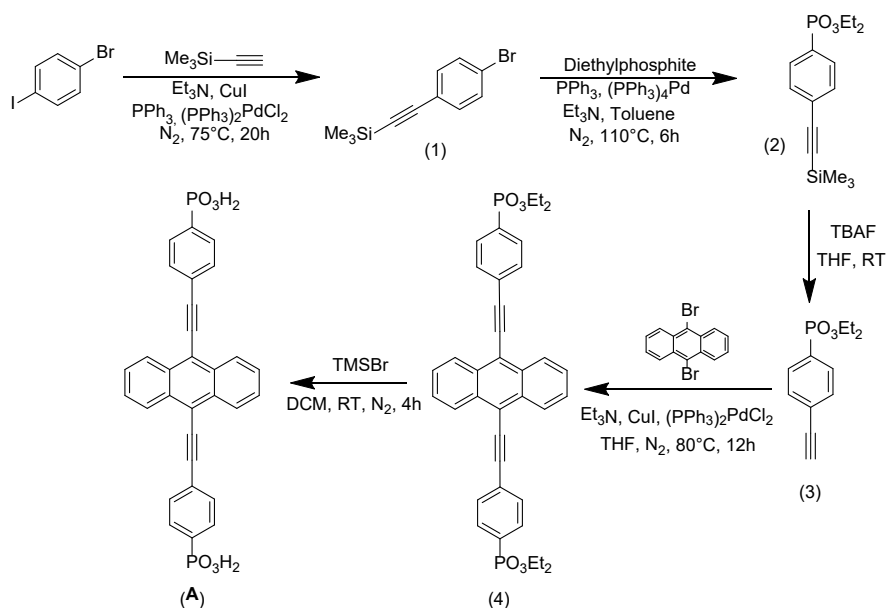


Figure S1: Synthesis of A.

((4-Bromophenyl)ethynyl)trimethylsilane (1)¹: To a 250 mL three-neck round bottom flask under N_2 atmosphere was added 80 mL of triethylamine, 6.70 g (23.7 mmol) of 1-bromo-4-iodobenzene, 0.087 g (0.3 mmol) of triphenylphosphine (PPh_3), 0.083 g (0.12 mmol) of bis-(triphenylphosphine)palladium chloride ($(\text{PPh}_3)_2\text{PdCl}_2$), and 0.108 g (0.6 mmol) of copper iodide (CuI). 3.36 mL (24.3 mmol) of ethynyltrimethylsilane was added dropwise to the solution as it was stirring and being heated to 75°C . The mixture was stirred for 20h at 75°C . When 20h had elapsed, the reaction flask was removed from heat and the solvent was removed under vacuum. The residue was dissolved in 75 mL of DCM and washed with DI water three times. The organic layer was collected and the solvent evaporated to form an off-white solid (**1**) used without further purification. Yield – 5.52 g, 92%. ^1H NMR (400 MHz, CDCl_3): δ (ppm) 7.45 (2H, dd, $J = 8.0$ Hz, 13.2 Hz); 7.34 (2H, dd, $J = 4.0$ Hz, 8.0 Hz); 0.27 (9H, s).

Diethyl [4-((trimethylsilyl)ethynyl)phenyl]phosphonate (2)¹: To a 150 mL three-neck round bottom flask under N₂ atmosphere was added 2.50 g (9.9 mmol) of **1**, 12.948 g (49.4 mmol) of PPh₃, 0.570 g (0.5 mmol) (PPh₃)₄Pd, and 1.55 mL (11.1 mmol) Et₃N. Next, 52 mL of Toluene was added. To the mixture was added 1.67 mL (13.0 mmol) of diethylphosphite dropwise. The reaction stirred at 110°C for 6h. When 6h had elapsed, the reaction flask was removed from the heat and allowed to cool to room temperature. The reaction mixture was filtered by vacuum filtration. The filtrate was washed three times with ammonium hydroxide diluted to a pH ~ 9 (1:1 v/v). Following this, the mixture was washed with water (1:1 v/v) three times and dried with Na₂SO₄. Finally, the solvent was evaporated under reduced pressure to obtain a yellow oil. The oil was purified via column chromatography using 3:1 hexanes:ethyl acetate. A pure yellow oil (**2**) was obtained. Yield – 2.57 g, 84%. ¹H NMR (400 MHz, CDCl₃): δ (ppm) 7.76 (2H, dd, J = 8.0 Hz, 13.2 Hz); 7.56 (2H, dd, J = 4.0 Hz, 8.0 Hz); 4.22 – 4.03 (4H, m); 1.34 (6H, t, J = 8.0 Hz); 0.28 (9H, s).

Diethyl (4-ethynylphenyl)phosphonate (3)¹: To a 150 mL three-neck round bottom flask under N₂ atmosphere was added a solution of 1.0 g (3.2 mmol) of **2** dissolved in 6.0 mL of dry THF. An additional 60 mL of THF was added to the flask. Then, 15 mL (15.0 mmol) of tetrabutylammoniumfluoride (1.0 M in THF) was added dropwise and the solution should go from yellow to red. The reaction is stirred for 45 minutes, then stopped, and the solvent evaporated. The residue was diluted in 30 mL of diethyl ether before washing three times with an equal volume of aqueous ammonium hydroxide diluted to pH ~ 9. The ethereal layer was dried over Na₂SO₄ and the solvent evaporated. The crude product was purified via column chromatography using a 1:1 v/v of hexanes:ethyl acetate. An orange/yellow oil (**3**) was collected. Yield – 0.58 g, 76%. ¹H NMR (400 MHz, CDCl₃): δ (ppm) 7.79 (2H, dd, J = 8.0 Hz, 12.0 Hz); 7.60 (2H, dd, J = 4.0 Hz, 8.0 Hz); 4.23 – 4.05 (4H, m); 3.23 (1H, s); 1.35 (6H, t, J = 8.0 Hz).

Tetraethyl ((anthracene-9,10-diylbis(ethyne-2,1-diyl))bis(4,1-phenylene))bis(phosphonate) (4)²: To a 100 mL three-neck round bottom flask under N₂ atmosphere was added 0.88 g (2.6 mmol) 9,10-dibromoanthracene, 73 mg (0.1 mmol) (PPh₃)₂PdCl₂, 30 mg (0.2 mmol) copper iodide, 35 mL of dry THF, and 6.0 mL Et₃N. The mixture was stirred for 15 minutes at room temperature before a solution of 1.25 g (5.3 mmol) of **3** dissolved in 10 mL of THF was added

dropwise. Following this addition, the temperature was increased to 80 °C for 20 h. After completion, the reaction was cooled to room temperature and the solvent evaporated under reduced pressure. The residue was dissolved in DCM and washed with DI water three times, followed by brine, dried over Na₂SO₄, and the solvent removed under reduced pressure. The crude product was purified via column chromatography with ethyl acetate as the eluent. A fluorescent green solution was eluted, the solvent evaporated, and an orange powder (**4**) was obtained. Yield – 0.72 g, 67%. ¹H NMR (400 MHz, CDCl₃): δ (ppm) 8.71 (4H, dd, J = 4.0 Hz, 8.0 Hz); 7.97 – 7.86 (8H, m); 7.71 (4H, dd, J = 4.0 Hz, 8.0 Hz); 4.29 – 4.08 (8H, m); 1.40 (12H, t, J = 4.0 Hz). ¹³C NMR (150 MHz, CDCl₃): δ (ppm) 132.19, 132.00, 131.93, 131.59, 131.49, 127.19, 127.14, 118.36, 101.54, 101.53, 88.99, 62.39, 62.35, 16.42, 16.38.

((Anthracene-9,10-diylbis(ethyne-2,1-diyl))bis(4,1-phenylene))bis(phosphonic acid) (A)³: To a three-neck, round bottom flask under N₂ atmosphere was added 100 mg (0.24 mmol) of **4** and 5 mL of dry DCM. The mixture was bubble degassed for 30 min and 700 μL (5.3 mmol) of bromotrimethylsilane was added dropwise. The mixture was stirred at room temperature for 4 h. After 4 hours, the reaction flask was placed in an ice bath to cool before 3 mL of cold DI water was added. An orange precipitate was formed, filtered, and dried. The product was washed with water 3 times to get pure **A**. Yield – 42.2 mg, 58%. ESI-MS (m/z): Calculated for C₃₀H₂₀O₆P₂ – 538.07, Observed – 537.06 [M - 1]⁺; ¹H NMR (400 MHz, DMSO-*d*₆): δ (ppm) 8.75 (4H, d, J = 4.0 Hz); 8.23 (4H, d, J = 4.0); 8.01 (4H, d, J = 6.0); 7.81 – 7.72 (4H, m). ¹³C spectrum could not be recorded due to poor solubility of the compound.

Photophysical and Electrochemical Measurements

Absorption Spectra: Data were recorded on an Agilent 8453 UV-visible photo diode array spectrophotometer. Thin film absorption spectra were obtained by placing dry, derivatized MO₂ (M = Zr or Ti) slides perpendicular to the detection of the beam path.

Nuclear Magnetic Resonance (NMR): ¹H were recorded using Bruker 400 MHz spectrometer and ¹³C NMR spectra were recorded on a Bruker 600 MHz spectrometer at room temperature. Chemical shifts for protons are reported in parts per million (ppm) relative to the respective residual solvent peaks. All NMR spectra were processed using MNOVA.

High-Resolution Mass Spectrometry (HR-MS): High-resolution mass spectra of **A** in DMSO/MeOH were recorded using an Agilent 6230 TOF MS in negative mode (-ESI).

Attenuated Total Reflectance-Fourier Transform Infrared Spectroscopy (ATR-FTIR): Attenuated total reflectance infrared spectra were recorded using a Bruker Alpha FTIR spectrometer (SiC Glowbar source, DTGS detector) with a Platinum ATR quickSnap sampling module (single reflection diamond crystal). Spectra were acquired from 850 to 1700 cm⁻¹ at a resolution of 4 cm⁻¹. All ATR-IR spectra are reported in absorbance with a blank versus atmosphere.

*Amperometric *i*-*t*:* Data were collected using a CH Instruments 630E electrochemical analyzer using a two-electrode configuration (TiO₂ working, Pt counter) held at 0 V applied potential. The samples were irradiated with an AM1.5 solar spectrum generated from a 300 W Xe arc lamp (Newport, 6258) enclosed in an Oriel Research Arc-lamp Housing (Newport, 67005) with the light output passed through an AM1.5 Global filter (Newport, 81094) or with a 635 nm laser (Aixiz, AIX-635-180T) for intensity dependent measurements. The light intensity was measured using a calibrated reference solar cell (Newport, 91150 V) for the Xe lamp, and an intensity meter (Ophir Vega 7Z01560) with a high sensitivity power sensor (Ophir Vega 3A-FS 7Z02628) to measure laser intensities. A Model T132 Shutter Driver/Timer (UniBlitz) coupled to a mechanical shutter (Vincent Associates, VS25) was placed between the light source and sample to control light (20 s)-dark (5 s) intervals over an 80 s time period.

Incident Photon to Current Efficiency: Data were collected with a CH Instruments 630E electrochemical analyzer using a two-electrode configuration (TiO₂ working, Pt counter) held at 0 V applied potential while monitoring the current. The samples were irradiated using the output from a housed Oriel Instruments 300 W Xe arc lamp (Newport, 6258) enclosed in an Oriel Research Arc-lamp Housing (Newport, 67005), single grating (1800 λ mm⁻¹, 250 nm blaze) Czerny–Turner monochromator every 5 nm at a 5 nm bandwidth. Intensities were measured at each wavelength using an Ophir Vega power meter (Ophir Vega 7Z01560) with a high-sensitivity power sensor (Ophir 3A-FS 7Z02628). Due to the low signal to noise ratio in the NIR region, the IPCE spectra were smoothed with a 10 adjacent point averaging.

Intensity Dependence: Current density versus excitation power density plots were recorded using a CH Instruments 630E electrochemical analyzer with the working electrode attached to the anode (TiO₂ multi-layer film on FTO glass) and counter and reference electrodes attached to the cathode (Pt-coated FTO glass) in a sealed cell arrangement with I⁻/I₃⁻ mediator electrolyte. A 635 nm laser (Aixiz, AIX-635-180T) was used as the excitation source. The output of the laser was passed through a variable neutral density filter (Edinburgh F-B01 laser mount), a 1 mm diameter iris (Newport ID-1.0) and then directed to the sample via a flip mirror. An intensity meter (Ophir Vega 7Z01560) with a high sensitivity power sensor (Ophir Vega 3A-FS 7Z02628) was used to measure laser intensities, and a Thor Labs BC106N-VIS beam profiler was used to determine the laser spot size. Threshold intensities were consistent across several devices.

Excitation events per second: The intensities, measured in mW cm⁻², were converted to excitations s⁻¹ cm⁻² using the equation $I_{ex} = \frac{I_{mW}}{1000} \times \frac{\%A(\lambda)}{E_J(\lambda)}$, where I_{ex} is the intensity given in excitations s⁻¹ cm⁻², I_{mW} is the intensity in mW cm⁻², $\%A(\lambda)$ is the absorptance of the film at the excitation wavelength, λ , and $E_J(\lambda)$ is the energy, in joules, of a photon of wavelength λ .

Steady-State Emission: Emission spectra were recorded at room temperature using an Edinburgh FLS980 fluorescence spectrometer. The samples were excited using the light output from a housed 450 W Xe lamp passed through a single grating (1800 l/mm, 250 nm blaze) Czerny-Turner monochromator and finally a 1 nm bandwidth slit. Emission from the sample was first passed through the appropriate long-pass colour filter, then a single grating (1800 l/mm, 500 nm blaze)

Czerny-Turner monochromator (1 nm bandwidth) and finally detected by a Peltier-cooled Hamamatsu R928 photomultiplier tube.

Time-Resolved Emission: Time-resolved emission traces were acquired using the same spectrometer as the steady-state emission measurements. The emission decay traces were acquired using time-correlated single-photon counting (TCSPC; 1024 channels; 100 ns window) with data collection for 10,000 counts. TCSPC excitation was provided by an Edinburgh EPL-445 ps pulsed light emitting diode (445 ± 10 nm, pulse width 100 ps) operated at 10 MHz.

Transient Absorption: Transient absorption measurements were performed using a HELIOS FIRE transient absorption spectrometer (Ultrafast Systems) coupled to a Vitara-S Coherent Ti:sapphire laser and amplified using a 1 kHz Coherent Revolution-50 pump laser. The resulting 5 mJ pulse (100 fs full width half max at 800 nm) was then split into a pump and probe beam. The pump was directed through an optical parametric amplifier (OPerA Solo from Coherent), then was passed through a chopper to minimize laser line scattering, and directed towards the sample with a resulting intensity of 7 mJ/cm^2 at 475 nm and 15 mJ/cm^2 at 650 nm. The probe beam was directed through a delay stage and a white light continuum was produced by a sapphire crystal (range 420–780 nm) The pump and probe beam were then overlapped on the sample. For solution measurements, deaerated DMSO was used, and continuous stirring was performed on the samples in a 2 mm cuvette during the measurement. For thin films, samples sealed in air-free MeCN were mounted in a clamp stage. Signal was then collected by a CMOS detector. Difference spectra and single wavelength kinetics were collected averaging 3 times and holding for 2 seconds, with an exponential point acquisition beginning with 0.001 ps steps and totaling to 200 points. Data was processed (chip and time-zero correction) using the Surface Xplorer software package from Ultrafast Systems. For solutions, fittings were performed using mono-exponential decays. For thin films, fittings were performed using biexponential decays (see equation in *Lifetime determination*).

NIR Emission: Near-infrared emission measurements of **O**s were carried out in a DMSO solution (0.2 mM) in a quartz cuvette perpendicular to the excitation light source. The spectrometer is composed of a Continuum Surelite EX Nd:YAG laser combined with a Continuum Horizon OPO (532 nm, 5–7 ns, operated at 1 Hz, beam diameter ~ 0.5 cm, 2.5–5 mJ/pulse) integrated into a

commercially available Edinburgh LP980 laser flash photolysis spectrometer system. Time-resolved NIR emission scans were passed through a TMS302-A monochromator (1800 grooves/mm grating) with a 300 mm focal length in Czerny Turner configuration and detected by a Near-Infrared detector (NIR-LP, InGaAs PIN photodiode) with a 900 nm – 1650 nm spectral response range (3 mm active area, 2MHz cut-off frequency, 100 ns response width). Detector outputs were processed using Edinburgh's L900 (version 8.2.3, build 0) software package, and the peak intensity values were tabulated every 10 nm from 850-1400 nm with 10 averages per detection wavelength ($\lambda_{\text{ex}} = 650 \text{ nm}$, 1 μs window).

Lifetime determination: Emission decay kinetics for the films were fit with a biexponential function $y = A_1 e^{-x/\tau_1} + A_2 e^{-x/\tau_2} + y_0$ using the Edinburgh software package and a weighted average lifetime was calculated using $\langle \tau \rangle = \sum A_i \tau_i^2 / \sum A_i \tau_i$.

Energy Level Calculations for Figure 1

The ground state reduction potential and excited state oxidation potentials of A^4 and Os^5 were acquired from literature. Redox potentials for TiO_2 and I^-/I_3^- were obtained from our previous publication.⁶

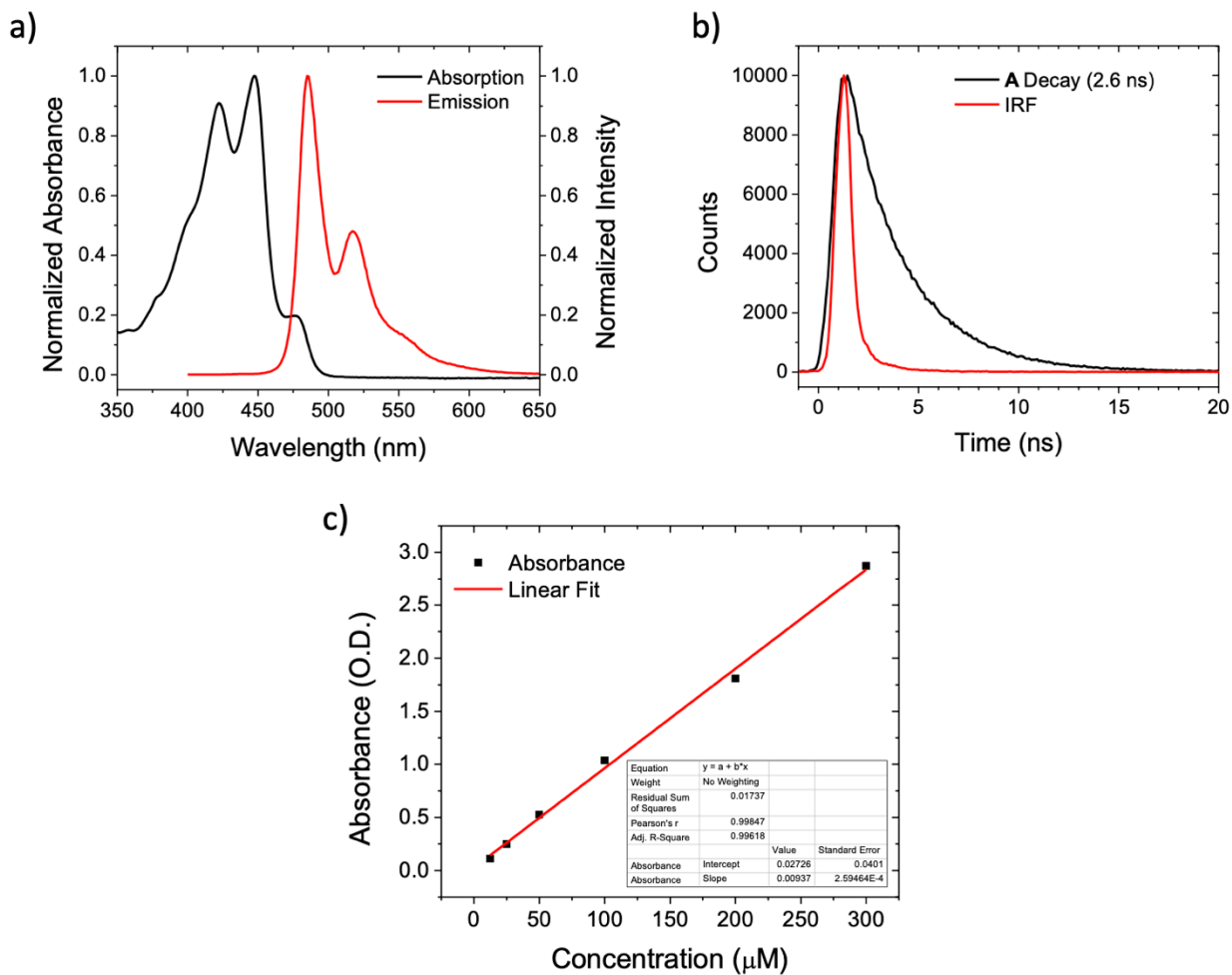


Figure S2. a) Normalized absorbance and steady-state emission ($\lambda_{ex} = 320$ nm, 375 nm LP), b) time-resolved emission ($\lambda_{ex} = 445$ nm, $\lambda_{em} = 485$ nm), and c) extinction coefficient calculation for A in DMSO.

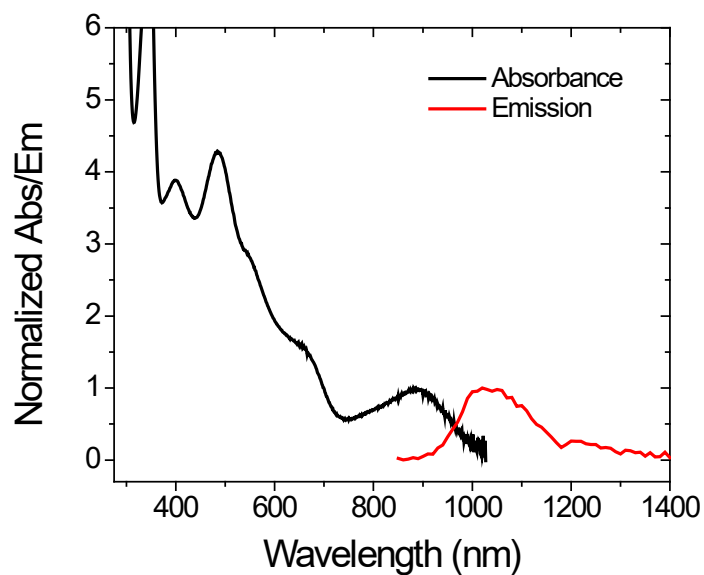


Figure S3. Normalized absorbance and emission ($\lambda_{\text{ex}} = 650 \text{ nm}$) spectra for **Os** in DMSO.

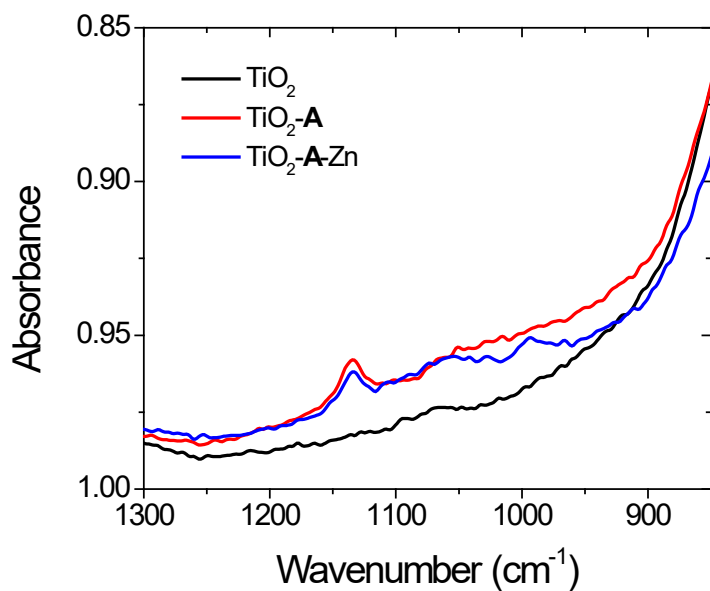


Figure S4. ATR-FTIR absorption spectrum of $\text{TiO}_2\text{-A}$ films before and after soaking in $0.5 \mu\text{M}$ $\text{Zn}(\text{OAc})_2$ in MeOH for 3 h.

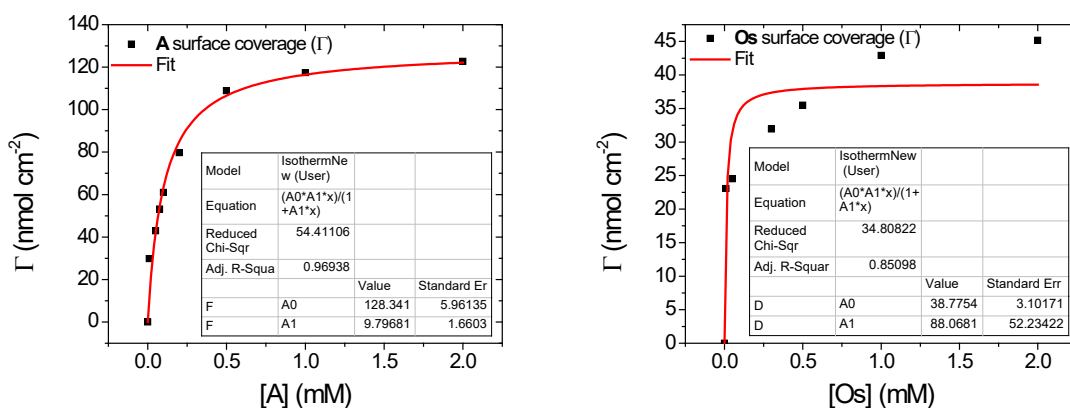


Figure S5. Surface coverage (Γ) isotherms for TiO_2 films immersed into **A** (left) in DMSO for 48 h from 0-2.0 mM and TiO_2 -**A**-Zn films immersed into **Os** (right) in 1:1 acetonitrile/tert-butanol for 24 h from 0-2.0 mM (all points are an average of two films).

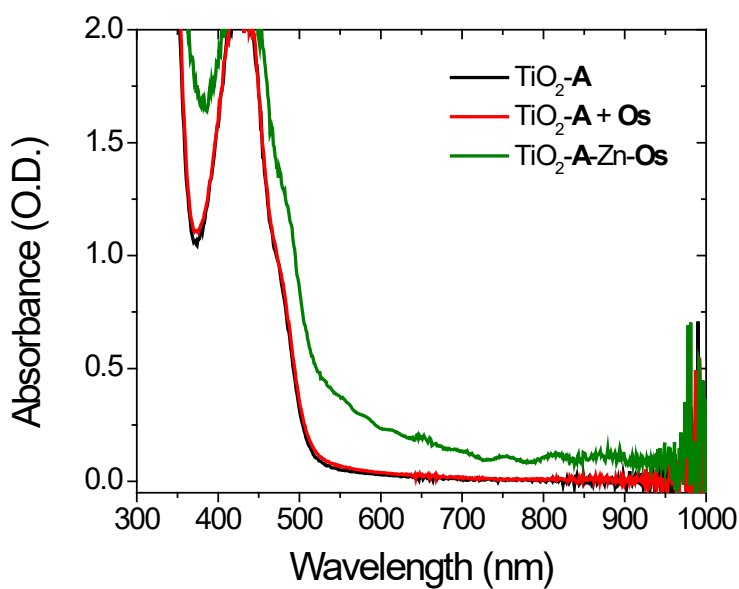


Figure S6. Absorption spectrum of TiO_2 -**A** films after soaking in 1 mM **Os** in 1:1 acetonitrile/tert-butanol for 24 h both with and without prior soaking in 0.5 μM $\text{Zn}(\text{OAc})_2$ in MeOH for 3 h.

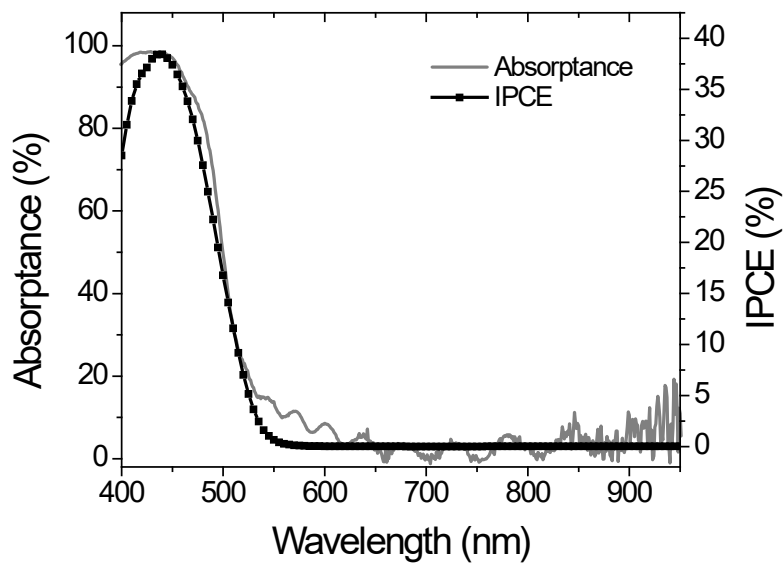


Figure S7. IPCE and absorbance spectra for TiO₂-A.

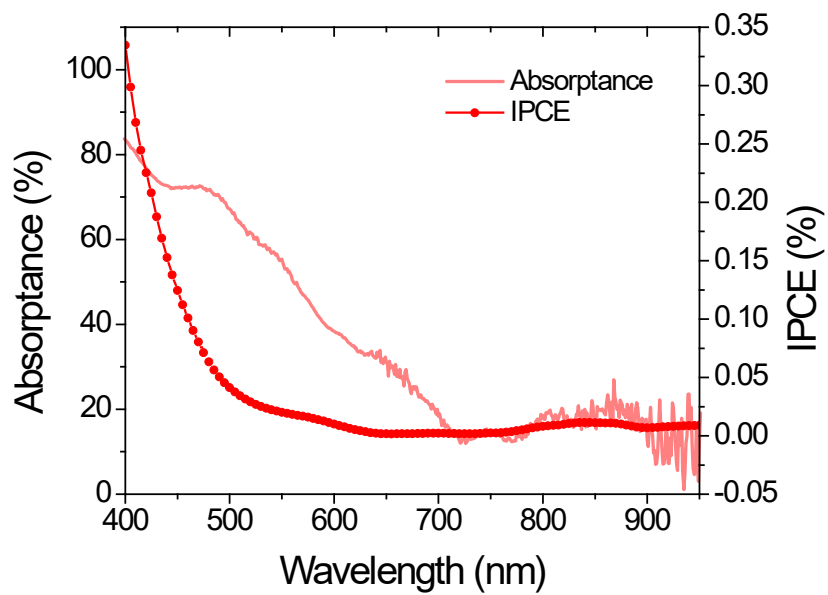


Figure S8. IPCE and absorbance spectra for TiO₂-B-Zn-Os.

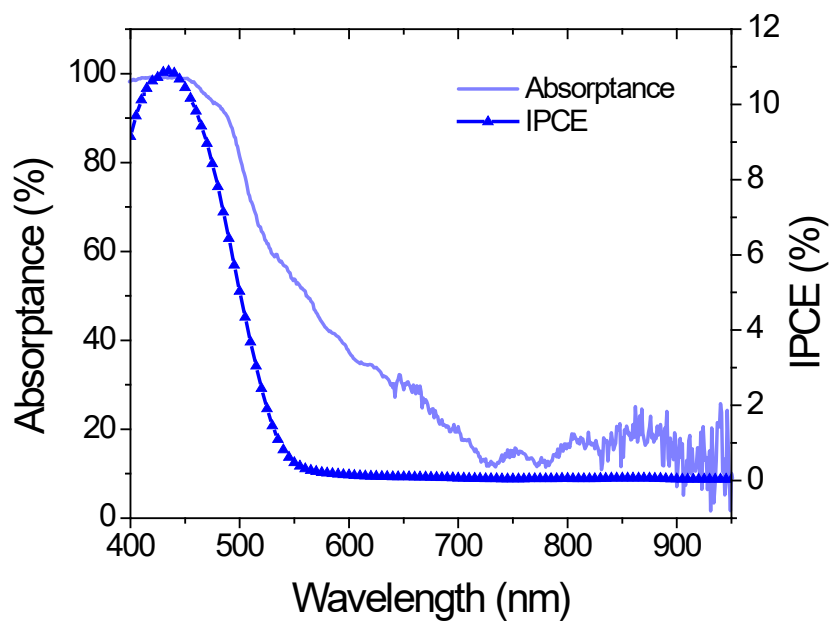


Figure S9. IPCE and absorbance spectra for $\text{TiO}_2\text{-A-Zn-Os}$.

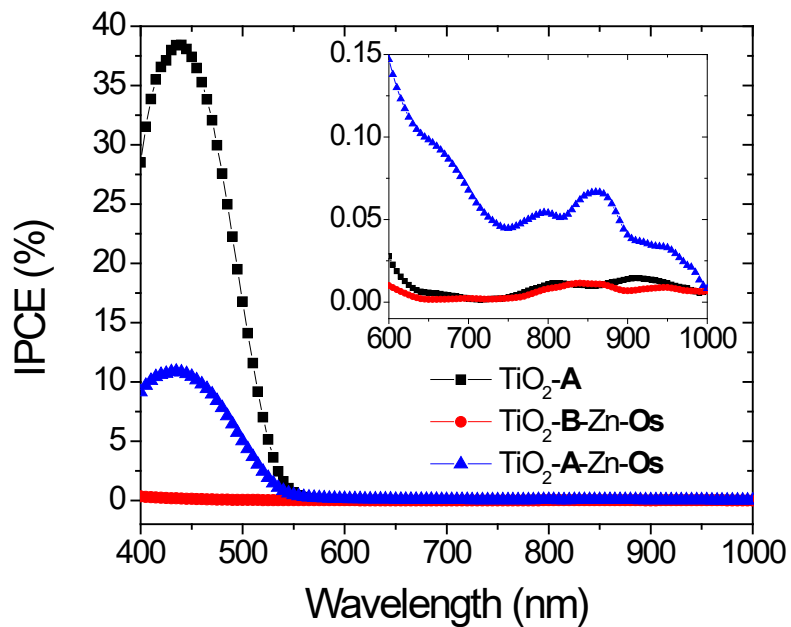


Figure S10. IPCE spectra for $\text{TiO}_2\text{-A}$, $\text{TiO}_2\text{-B-Zn-Os}$, and $\text{TiO}_2\text{-A-Zn-Os}$.

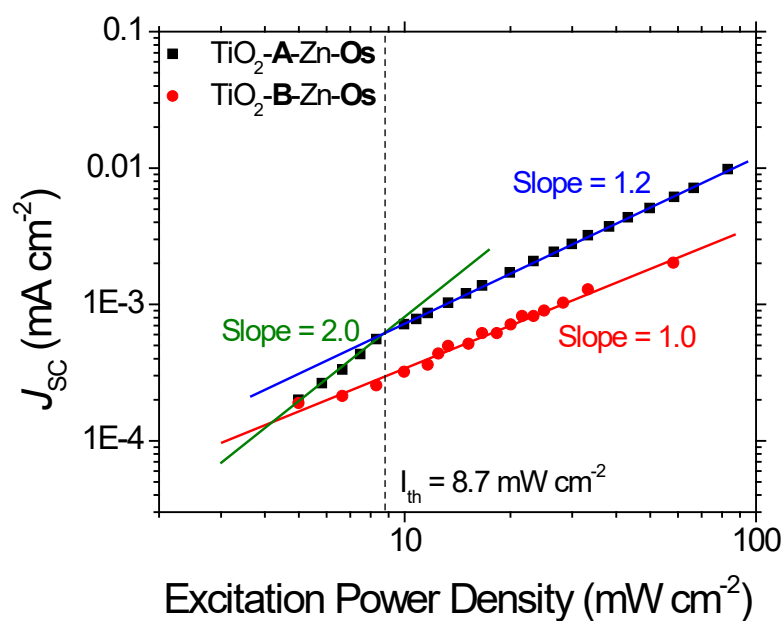


Figure S11. J_{SC} with respect to the excitation power density for bilayer devices ($\lambda_{ex} = 635$ nm).

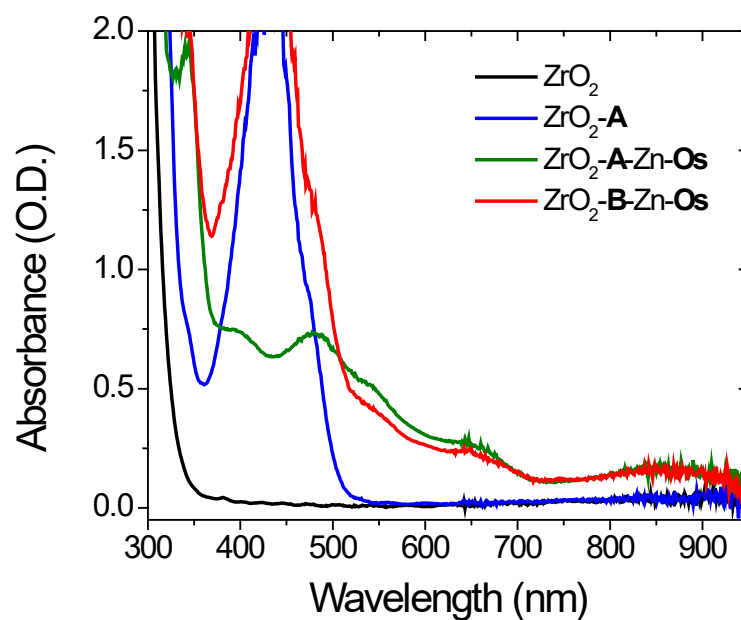


Figure S12. Absorbance spectra of monolayer and bilayer films on ZrO_2 .

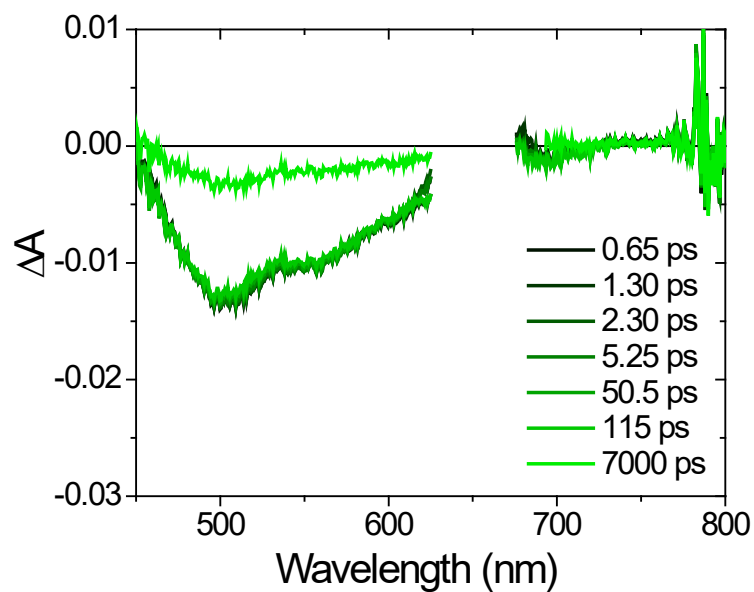


Figure S13. Transient absorption spectra of **Os** in DMSO ($\lambda_{\text{ex}} = 650$ nm).

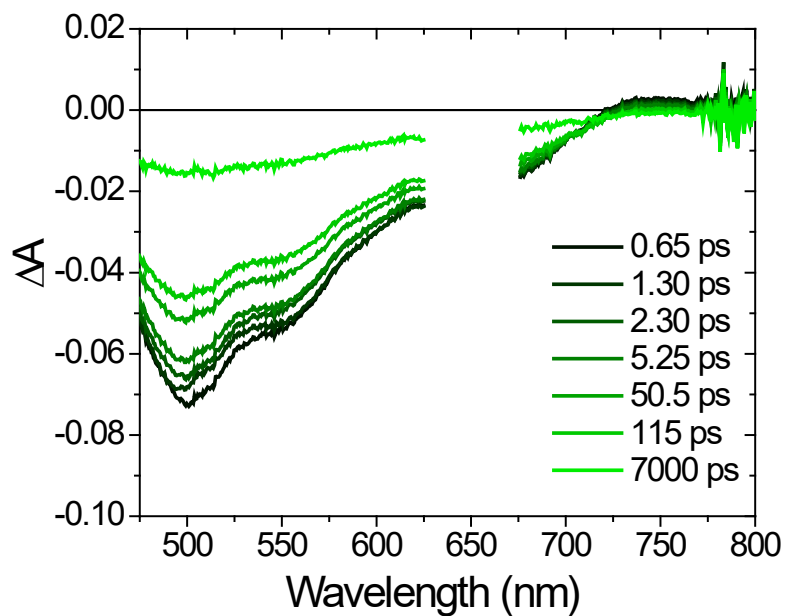


Figure S14. Transient absorption spectra of **TiO₂-Os** in dry MeCN ($\lambda_{\text{ex}} = 650$ nm).

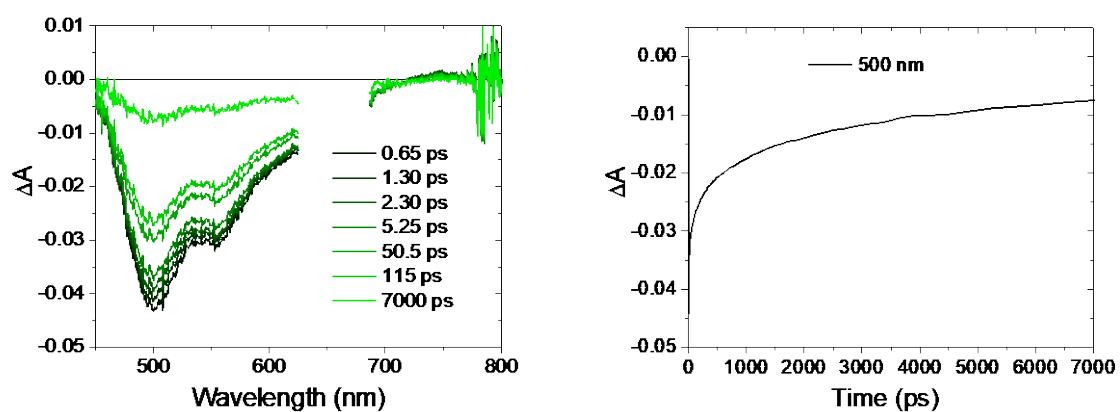


Figure S15. Transient absorption spectra (left) and kinetic absorption (right) of $\text{TiO}_2\text{-B-Zn-Os}$ in dry MeCN ($\lambda_{\text{ex}} = 650 \text{ nm}$, $\tau = 1.2 \text{ ns}$).

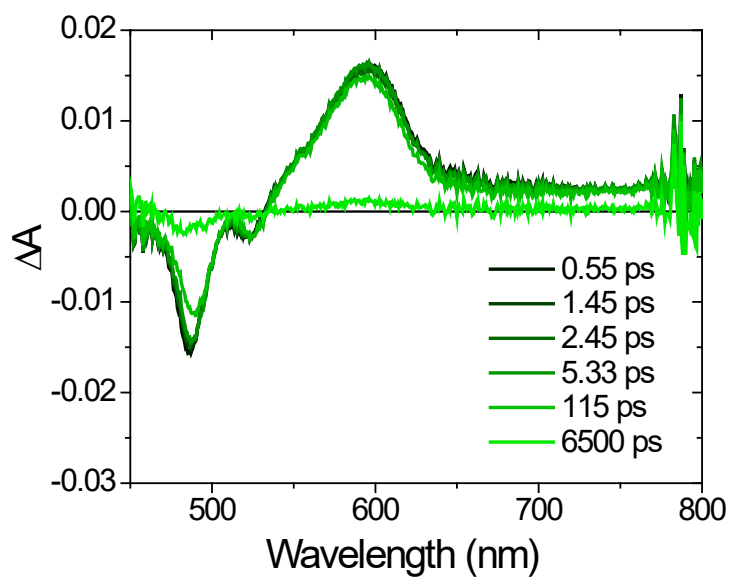


Figure S16. Transient absorption spectra of A in DMSO ($\lambda_{\text{ex}} = 475 \text{ nm}$).

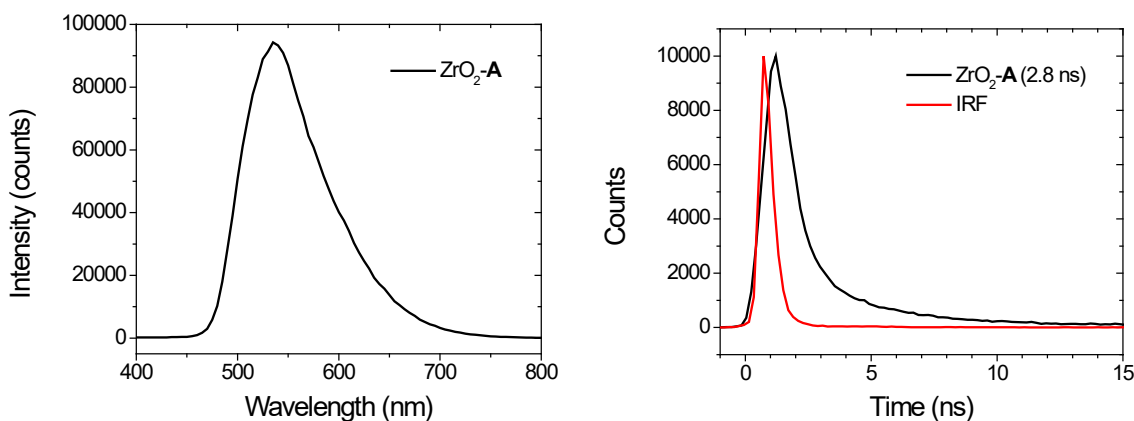


Figure S17. Steady-state (left, $\lambda_{\text{ex}} = 395$ nm, 420 LP) and time-resolved (right) emission spectra of $\text{ZrO}_2\text{-A}$ in dry MeCN ($\lambda_{\text{ex}} = 445$ nm, $\lambda_{\text{em}} = 535$ nm).

References

1. Onouchi, H.; Maeda, K.; Yashima, E., *J. Am. Chem. Soc.* **2001**, *123* (30), 7441-7442.
2. Yu, F.; Zhang, Y.-M.; Guo, Y.-H.; Li, A.-H.; Yu, G.-X.; Li, B., *CrystEngComm* **2013**, *15* (41), 8273-8279.
3. Hill, S. P.; Banerjee, T.; Dilbeck, T.; Hanson, K., *J. Phys. Chem. Lett.* **2015**, *6* (22), 4510-4517.
4. Simpson, C.; Clarke, T. M.; MacQueen, R. W.; Cheng, Y. Y.; Trevitt, A. J.; Mozer, A. J.; Wagner, P.; Schmidt, T. W.; Nattestad, A., *Phys. Chem. Chem. Phys.* **2015**, *17* (38), 24826-24830.
5. Altobello, S.; Argazzi, R.; Caramori, S.; Contado, C.; Da Fré, S.; Rubino, P.; Choné, C.; Larramona, G.; Bignozzi, C. A., *J. Am. Chem. Soc.* **2005**, *127* (44), 15342-15343.
6. Ogunsolu, O. O.; Murphy, I. A.; Wang, J. C.; Das, A.; Hanson, K., *ACS Appl. Mater. Interfaces* **2016**, *8* (42), 28633-28640.